



HAL
open science

A comprehensive methodology to support decision-making for additive manufacturing of short carbon-fiber reinforced polyamide 12 from energy, cost and mechanical perspectives

Thibault Le Gentil, Daniel Therriault, Olivier Kerbrat

► To cite this version:

Thibault Le Gentil, Daniel Therriault, Olivier Kerbrat. A comprehensive methodology to support decision-making for additive manufacturing of short carbon-fiber reinforced polyamide 12 from energy, cost and mechanical perspectives. *International Journal of Advanced Manufacturing Technology*, 2023, 10.1007/s00170-023-11161-2 . hal-04077022

HAL Id: hal-04077022

<https://hal.science/hal-04077022>

Submitted on 21 Apr 2023

HAL is a multi-disciplinary open access archive for the deposit and dissemination of scientific research documents, whether they are published or not. The documents may come from teaching and research institutions in France or abroad, or from public or private research centers.

L'archive ouverte pluridisciplinaire **HAL**, est destinée au dépôt et à la diffusion de documents scientifiques de niveau recherche, publiés ou non, émanant des établissements d'enseignement et de recherche français ou étrangers, des laboratoires publics ou privés.

A comprehensive methodology to support decision-making for additive manufacturing of short carbon-fiber reinforced polyamide 12 from energy, cost and mechanical perspectives

Thibault Le Gentil^{1,2}, Daniel Therriault^{2†} and Olivier Kerbrat^{1*†}

^{1*}Civil and Mechanical Engineering Institute, CNRS GeM, Rennes University, Rennes, France.

²Laboratory for Multiscale Mechanics (LM2), Department of Mechanical Engineering, Polytechnique Montreal, Montreal, Quebec, Canada.

*Corresponding author(s). E-mail(s): olivier.kerbrat@ens-rennes.fr;

Contributing authors: thibault.le-gentil@ens-rennes.fr; daniel.therriault@polymtl.ca;

†These authors contributed equally to this work.

Abstract

Additive manufacturing (AM) technologies have transformed manufacturing, by providing greater control over material deposition and consumption. Thanks to greater customization and their high strength-to-mass ratio, AM of composite materials has significantly grown over the past few years. The main focus in research area are is improving printing precision and higher production rates. However, there is a lack of thorough analysis on the energy consumption of Fused Filament Fabrication (FFF) machines for composite manufacturing, especially when associated to mechanical and economic aspects. We designed an experimental method, based on flow analysis for measuring the impact of temperature parameters on total cost, energy consumption, and tensile resistance of composite parts made by FFF. As the user should be able to improve FFF efficiency regarding economic, energy and technical aspects and obtain recommendations for setting up and using the machine. This study confirms that combining traditional economic and technical indicators (total cost and tensile resistance) to emerging energy indicators (specific energy consumption) can be successfully applied to additive manufacturing to provide an overview of printing parameters impact. Results are yielding information to support optimization investigations depending on the need and goal. For example, two tested parameter combinations that offer similar tensile properties (4% reduction in tensile resistance compared to best combination) show a 20% difference with a lower energy consumption

Keywords: Fused filament fabrication, Manufacturing cost, Energy consumption, Energy model, Multiple-criteria decision analysis, Polymer composites

1 Introduction

Additive manufacturing (AM) has attracted interest from both academia and industry, on account of its numerous applications in a variety of fields

[1]. Contrary to a traditional manufacturing process, AM refers to a family of manufacturing techniques in which three-dimensional components are fabricated by adding materials layer-by-layer. The increased demand on more complex

products and designs in a more efficient and sustainable way reflects some of the advantages of AM. The trend in both industry and research is to take advantage of the geometry freedom to produce lighter parts while keeping similar mechanical properties for composite and metallic parts [2–4]. These advantages includes a higher flexibility in both design and supply chain, and allows parts to be made that are impossible to produce in conventional manufacturing [5]. Additionally, for extrusion-based AM processes, this flexibility helps reduce raw material consumption and material waste [6]. Therefore, in the context of Industry 4.0 and sustainability, AM is seen as one of the many means of bringing about this transition [2]. Among the AM processes, fused filament fabrication (FFF) the most widespread AM technique, has found applications within various sectors including aerospace, automotive, sport, and construction [7]. In particular, the combination of AM and carbon-fiber-reinforced polymer opens up the possibility of producing parts with a high stiffness-to-weight ratio [8], whilst reducing total mass through complex designs [9].

Thanks to recent technological progress, many materials are now applied to AM. Polyamide 12 (PA12) found many applications due to its high ductility (elongation at break up to 10% for FFF printed part [10]) and high toughness (about 500 MJ/m³ [11, 12]), with relative low cost. Additionally for the case of aerospace or automobile, PA12 respect flame resistance standards [13]. While, PA12 might be limited to relative low strength resistance, the addition of carbon fiber greatly enhance mechanical properties of the material, mainly stiffness-to-weight ratio [14]. Short carbon-fiber reinforced polyamide 12 (PA12-CF) have been used to form lightweight aerospace non-structural applications and automotive parts [13]. Moreover, the mechanical properties and printability of the PA12-CF filament varies with printing parameters or AM technology [15]. Table 1 compiles mechanical properties of PA12 and PA12-CF for virgin material and the two main AM process FFF and Selective Laser Sintering (SLS), with FFF PA12-CF showing higher mechanical resistance with a large variation depending on the carbon weight percentages used.

Regarding sustainability, AM has several potential drawbacks, for examples material’s high

embodied impacts and recyclability [28]. Specifically, related to the printing process, there are two major issues, the first being the high energy demand during the manufacturing phase, and the second, the reduced productivity, compared to conventional processes [29–31]. Given the rapid growth of AM in industry, and the importance of ensuring sustainable development, there is a real need to investigate the relationship between energy consumption, cost, and the quality of the produced parts. In the present study, we therefore sought to develop a methodology for connecting these three aspects in the case of FFF of PA12-CF. After reviewing the relevant literature on energy and cost assessment in AM (Section II), we describe the methodology we used to model the process and acquire the relevant data (Section III). Then we present the design of experiments based on the fabrication of tensile specimens (Section IV). Two printing parameters are varied (printhead temperature and heated bed strategy) on three levels each in order to obtain energy consumption, mass and tensile test. Results are then compiled in economic (total cost), energetic (Specific Energy Consumption and Specific Printing Energy) and mechanical (tensile resistance and Young’s modulus) indicators (Section V), followed by a discussion (Section VI) and conclusion (Section VII).

2 Relevant literature on energy and cost assessment

2.1 Energy assessment and specific energy consumption of FFF

Initially designed for subtractive processes by Kara and Li [32], the specific energy consumption (SEC) indicator has since been applied to AM as a way of comparing and quantifying the energy efficiency of different processes or machines. SEC is defined as the ratio of total energy consumption to the mass deposited, and can be used to quantify energy efficiency in material deposition. Liu & al. [33] examine SEC values for different AM processes and their relation to global warming potential hence, creating a connection from energy consumption to a more global Life Cycle Assessment (LCA). This study also shows the opportunity to increase energy efficiency without

Table 1 Compilation of available data on mechanical properties of virgin PA12, PA12 by SLS and FFF, and PA12-CF by SLS and FFF. *Note : NA for Non Applicable.*

Material	Process	Filler	Mechanical properties					Source
			Tensile strength [MPa]	Young modulus [GPa]	Flexural strength [MPa]	Flexural modulus [GPa]	Tensile Elongation at break [%]	
PA12	Virgin	NA	53	1.8	68	1.7	200	Ensinger Plastics [16]
			43	1.4	44	1.2	350	Evonik [17]
	SLS	NA	-	-	53.9	1.54	-	[18]
			42.5	0.86	68	-	1.4	[19]
			35	0.9	-	1.5	-	[20]
FFF	NA	61	0.53	42	1.06	439	[21]	
		54	0.94	32	0.84	-	[22]	
		-	-	-	-	-	[23]	
PA12-CF	SLS	30% wt	-	-	74	3	-	[23]
		33% wt	66	6.3	-	-	5	[24]
	FFF	10% wt	94	3.6	125	5.26	8	[25]
		6% wt	33.5	1.85	55.3	0.31	-	[26]
		35% wt	89	5.2	-	-	-	[14]
		<20% wt	63	3.8	84	3.75	3	3DXTech [27]
		-	-	-	-	-	-	-

compromising the print quality. Dunaway & al. [34] studied experimentally the relation between energy consumption and part geometry characteristics. When Lunetto and al. compiled all the available SEC data in the literature [29], they found significant variability in energy efficiency, ranging from 19 MJ/kg to 1247 MJ/kg for polymers. This variability can be explained by the differences in SEC, depending on the printer's architecture (e.g., type, enclosure), the materials, the process parameters, and the geometric complexity. The warming up of the heating elements has been identified as the main demand of power [35]. The warm-up phase greatly varies depending on the printer architecture or the working environment (i.e., room temperature, humidity). Hence a second indicator, specific printing energy (SPE; i.e. SEC during the deposition phase), can be determined to focus on the printing phase. Total energy consumption can be divided into two categories: energy for the preparation of the printing (E_p), and energy directly needed for the fabrication phase (E_f).

2.2 Cost assessment

The modeling of cost with environmental consideration helps framing decision-making during manufacturing [36]. Many types of cost models exists regarding printing a single part, sometimes specific to a process or a material [37–40]. Still, six distinct cost categories can be identified: 1) materials (including supporting material); 2) electricity (e.g., warm-up, build-up, calibration); 3) workforce (software and hardware); 4) pre- and

postprocess (including quality control); 5) indirect cost (e.g., investment, maintenance); and 6) consumables. The total cost C_{tot} of manufacturing is estimated as follows:

$$C_{tot} = C_{materials} + C_{electricity} + C_{workforce} + C_{pre/post\ process} + C_{indirect} + C_{consumables} \quad (1)$$

One of the main advantages of AM compared to conventional manufacturing is *complexity-for-free*. AM does not rely on specific moulds or tools to manufacture part, which implies that the production cost does not rely on the complexity of the design, easing the production of lightweight parts [41].

2.3 Coupling aspects

Approach combining economic, energy and technical aspects to support decision-making are necessary to evaluate printing efficiency. Yosofi & al. [42] proposed a holistic approach for evaluating a part produced by an AM process regarding surface roughness, material, electrical and fluid consumption. Gutierrez-Osorio & al. [43] compared SEC, Young's modulus and tensile strength as a function of the layer thickness for different AM process. However based on literature review, a gap in comprehensive investigations on process energy consumption and print quality still exists.

2.4 Motivation for the present approach

In the literature, energy and cost assessments have mainly focused on the AM of polymer. In the case of composite materials, especially fiber-reinforced polymers, the demand for high performance and high mechanical properties requires the produced parts to be assessed from a mechanical perspective. Hence, there is a need to analyze the technical, economic and environmental impact of printing parameters for the AM of fiber-reinforced composites. The method we devised is based on a flow analysis of the manufacturing phase. This analysis yields an overview of the different parameters involved in the process, allowing optimization solutions to be explored. First, establishing the total manufacturing cost gives an indication of the parameters that can be modified and optimized from an *economic point-of-view*. Those modifications have impacts that need to be assessed from an *environmental point-of-view*. Finally, to ensure the industrial viability of the process, the impact on mechanical performance needs to be measured from a *mechanical point-of-view*.

3 Modelling approach

3.1 Flows

A cradle-to-gate representation of the material and energy flows involved in FFF of composite material is provided in Figure 1. Cradle-to-gate correspond to the lifecycle of the product, from the raw materials to the final product. This schematic shows that the process encompasses a wide range of subprocesses that are all interconnected and influence each other. There is still a lack of knowledge regarding the influence and the interconnection between each subprocesses, in terms of economic, environmental, and mechanical aspects. For a gate-to-gate approach, where only the pre-manufacturing and manufacturing steps are considered (in green on Figure 1), the storage of the material and file creations are the first steps. Regarding the FFF machine, manufacturing a part can be divided in two subprocesses : first, warming-up of the different heating elements (i.e., preparation subprocess related to E_p), and

second, the deposition of the part (i.e., fabrication subprocess related to E_f).

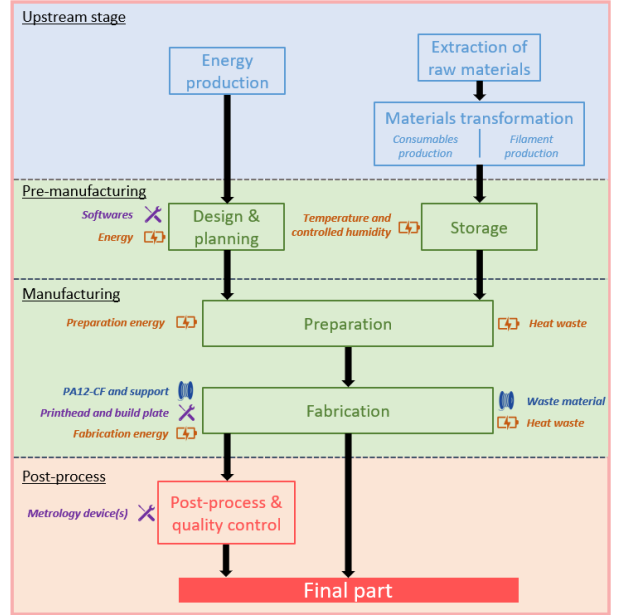


Fig. 1 Production line of FFF printing with flow representations (energy flows in orange, resources flows in blue, and consumables flows in purple). Green background represents the focus of the article on manufacturing; blue background is upstream process and red background is potential downstream.

3.2 Cost model

Coupling the flow model of Figure 1 with the previously identified cost categories enable to obtain a generic formula for the total cost (see variables definitions in Table 2):

$$\begin{aligned}
 C_{\text{tot}} = & C_{\text{part}} \times M_{\text{part}} + C_{\text{sup}} \times M_{\text{sup}} \\
 & + C_{\text{elec}} \times (P_p \times t_p + P_f \times t_f) \\
 & + C_{\text{op,hard}} \times (t_f + t_{\text{post}}) + C_{\text{op,soft}} \times t_{\text{soft}} \\
 & + \frac{C_{\text{soft}}}{t_{\text{soft}}} + \frac{C_m}{t_{hr} \times \beta} + \frac{M}{t_f + t_p} \\
 & + \sum_1^N C_{\text{cons}} \frac{t_{\text{cons}}}{T_{\text{cons}}}
 \end{aligned} \tag{2}$$

The Eq. 2 consider the six categories established in Eq. 1, and the entirety of the process.

Table 2 Nomenclature of the different variables and their associated definitions and unit.

Variables	Definitions [Unit]	Variables	Definitions [Unit]
C_{tot}	Total cost [€]	C_{man}	Cost for manufacturing scope [€]
C_{part}	Base material part cost [€/kg]	C_{sup}	Support cost [€/kg]
M_{part}	Base material part mass [kg]	M_{sup}	Support mass [kg]
C_{elec}	Base electricity cost [€/Whr]	t_p	Preparation time [hr]
P_p	Preparation power [W]	t_f	Fabrication time [hr]
P_f	Fabrication power [W]	$C_{\text{op,hard}}$	Hardware operator cost [€/hr]
$C_{\text{op,soft}}$	Software operator cost [€/hr]	t_{post}	Post-process time [hr]
t_{soft}	Software (slicing and CAD) time [hr]	C_m	Machine cost [€]
M	Maintenance cost [€]	α	Machine lifetime [hr]
t_{hr}	Annual working hours [hr]	β	Percentage of use time [%]
N	Total number of consumables	$C_{\text{printhead}}$	Printhead cost [€]
$t_{\text{printhead}}$	Use time of the printhead [hr]	$T_{\text{printhead}}$	Printhead lifetime [hr]
t_{heatbed}	Use time of heatbed [hr]	T_{heatbed}	Heatbed lifetime [hr]
C_{heatbed}	Heatbed cost [€]		

However in most cases, the parameters cannot all be modified separately. With regards only on manufacturing scope, certain parameters are out of scope. In this case, the global equation (Eq. 2) is replaced by the gate-to-gate scope such as :

$$C_{\text{man}} = C_{\text{materials}} + C_{\text{electricity}} + C_{\text{consumables}} \quad (3)$$

$$\begin{aligned} C_{\text{man}} = & C_{\text{part}} \times M_{\text{part}} + C_{\text{sup}} \times M_{\text{sup}} \\ & + C_{\text{elec}} \times (P_p \times t_p + P_f \times t_f) \\ & + C_{\text{printhead}} \times \frac{t_{\text{printhead}}}{T_{\text{printhead}}} \\ & + C_{\text{heatbed}} \times \frac{t_{\text{heatbed}}}{T_{\text{heatbed}}} \end{aligned} \quad (4)$$

The Eq. 4 presents the different factors an operator can modify during the fabrication phase, namely the material, electricity, and consumables (here, printhead and heatbed). The material cost remains constant for the desired part design, and the consumables cost is only related to printing duration. Consequently, the electricity cost is the only variables that can be indirectly controlled by the operator through printing parameters. Divided into preparation (p) and fabrication (f) consumptions, those two phases depend on the

power demand (P_p , P_f) and the duration (t_p , t_f). Reducing these variables through printing parameters (e.g., temperature) can reduce the total cost.

3.3 Energy model

In the context of transition into a more sustainable industry, it is particularly crucial to consider the impact of decisions on energy consumption. SEC is an interesting quantitative indicator of total electricity consumption during the manufacturing phase. Additionally, the power profile can give qualitative information about the distribution of the power demand. Figure 2 provides an example of power profiles plotted as a function of process time for PA12-CF. Six different process phases can be identified: 1) idle and file launching; 2) heatbed warm-up; 3) printhead warm-up; 4) calibration and printing; 5) end and return to 0; and 6) idle. Phases 2) and 3) are temperature (hence material) dependent while Phase 4) is design dependent, finally, Phases 1), 4) and 6) are operator dependent. The preparation energy corresponds to the sum of the switch-on, file launch, heating (heatbed and printhead), calibration, return to 0 and idle phases. While fabrication energy corresponds to the energy used to keep the elements warm and displace them. As shown in Figure 2, the terms for fabrication energy E_f are directly given by the power demand in Phase 4), without the need to individually measure each displacement or heating energy term. Additionally,

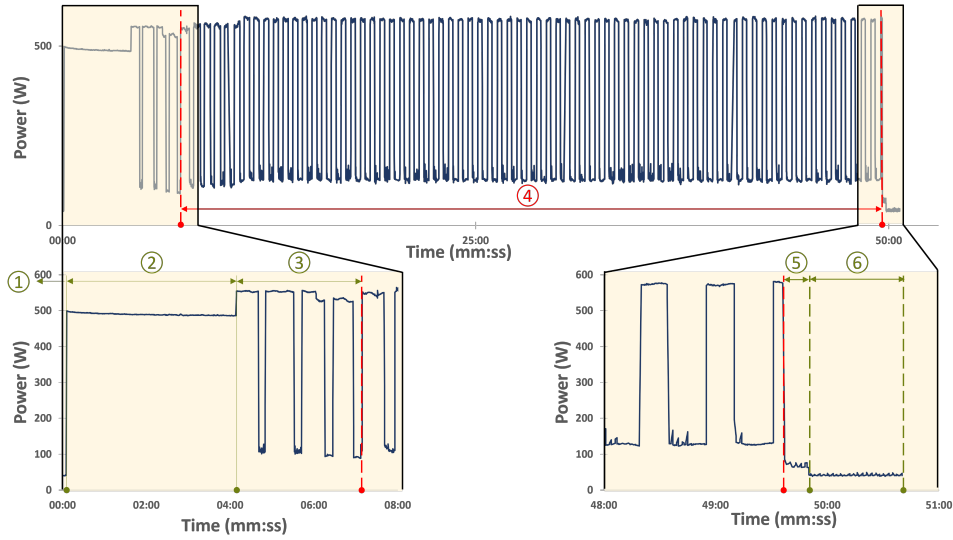


Fig. 2 Power profile and identification of main printing phases. This profile corresponds to the printing of a specimen A1, PA12-CF at 260 °C printhead and 100% heating at 80 °C for the heatbed. Steps 1-3, 5 and 6 are preparation steps (green periods). Step 4 is fabrication (red period).

the energy consumption for the warm-up and E_f are related to the temperatures of the printhead and the heatbed.

3.4 Mechanical performance

Carbon-fiber-reinforced polymer can be used in AM to improve material properties, thus, even with energetic consideration it is essential to control the quality of the part. In particular, if replacing a metallic part with a composite one means a drastic loss in mechanical performances, any reductions in cost and energy are irrelevant. Hence to ensure industrial viability, mechanical property needs to be assessed.

4 Experimental methods

4.1 Materials and equipment

We used a Raise 3D Pro2 FFF printer, an enclosed printer. To assess the mechanical properties of the printed part, we selected a tensile specimen Type A1, from standard ISO 527-2:2012. The filament material was CarbonXTM Nylon-CF Gen 3 from 3DXTech, with 240-270 °C and 80-110 °C as recommended temperatures from the manufacturer for the nozzle and the heatbed, respectively. Filament was stored in a vacuum oven to control humidity. We used a Fluke 289 multimeter to

measure the electrical current during manufacturing. Mass of printed part are directly measured at the end of manufacturing. The voltage was measured upstream and assumed to remain constant throughout the experiment. Tensile tests were performed on Instron 1362 testing system with a 5kN load cell. Speed of testing is 5 mm/min, ultimate tensile resistance and Young's modulus are calculated following ISO 527-1:2012.

4.2 Design of experiment

To illustrate the impact of printing parameters on energy consumption and cost, as seen with Eq. 3, we selected two factors: printhead temperature, and heatbed heating strategy. Deposition orientation and infill were also considered, as they are common variables in FFF manufacturing. However, on one hand, the best tensile resistance for CRFP will always be delivered throughout the filament orientation without affecting energy consumption. On the other hand, for tensile specimen, an infill of 100 % must be chosen for optimal performance.

From the recommended temperature, we selected 245 °C, 250 °C, and 260 °C as our values for the nozzle temperature and the lower limit for the heatbed temperature 80 °C. To minimize energy consumption, one could select a temperature below the recommended temperature,

however, capability of the print is not ensured anymore. For the second parameter, we chose three levels depending on the number of heated layers relatively to the total number of layers printed (in percentage): full heating of the heatbed (100%), heating stopped at half the total layers (50%), and no heating (0%). In total, we performed nine different tests, with four repetitions for each condition. Tables 3 and 4 lists both fixed and variables printing parameters. In the case of Experiments #1 and #4, the adhesion between the part and the heatbed does not allow a proper deposition of the materials. This indicates threshold temperature conditions below which proper adhesion and deposition are difficult.

Conditions #1, #4 and #6 have the same printing parameters, except printhead temperature. Condition #1 can not be successfully printed, meaning a 245 °C printhead temperature coupled with 0 % heatbed are insufficient. For condition #4, $T_P = 250$ °C and 0 % heatbed strategy are at the limit of the capability for the printer. Other conditions are within the range of capability of the printer and the variability is in terms of performance.

Table 3 Printing parameters held constant throughout the experiment.

Constant parameter	Value	Unit
Deposition speed	80	mm/s
Heatbed temperature (T_H)	80	°C
Layer thickness	0.2	mm
Outline shell	1	-
Infill percentage	100	%
Nozzle diameter	0.4	mm
Deposition orientation	+/- 45	°

Table 4 Variables and design of experiment.

Condition #	Printhead temperature T_P [°C]	Heatbed strategy [%]
1	245	0
2	245	50
3	245	100
4	250	0
5	250	50
6	250	100
7	260	0
8	260	50
9	260	100

5 Results

5.1 Cost data

Total cost and cost distribution between materials, electricity and consumables are shown in Figure 3. Associated constant parameters are defined in Table 5. Materials represented the main cost, ranging from 74% to 94% of the total cost, depending on the conditions. As material consumption was roughly the same across all experiments, the absolute value of the material cost remained constant. It was therefore the differences in energy consumption that were responsible for the changes in total cost. From the conditions without heatbed heating to conditions with full heating, differences in power demand meant that the electricity cost represented between 5% and 20% of the total cost. As printing duration was equal for each experiment, the cost of consumables was not affected.

5.2 Energy data

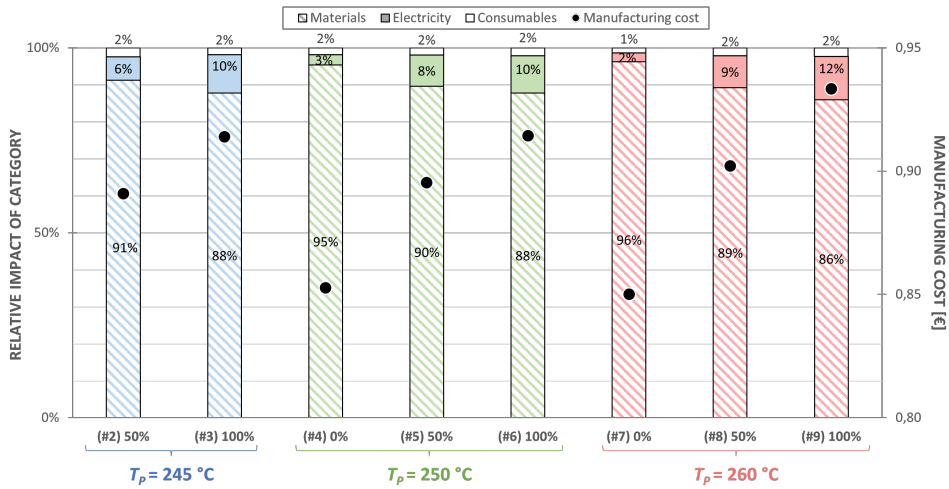
Figure 4 shows the different results of SEC (all six phases described in Figure 2), and SPE (Phase 4 only). As expected, energy consumption increased as the temperature increased. The difference in energy was, however, smaller between 50% and 100% than between 0% and 50%.

5.3 Tensile test data

Each of the 36 tensile specimens was mechanically tested, without any post-process. Figure 5 show results of each experiment regarding Young's modulus and ultimate tensile strength (UTS). Results revealed a substantial drop-off for experiments without heatbed heating (#4 and #7) on both Young's modulus and UTS. Young's modulus is relatively constant for experiments when heatbed strategy is 50 % or 100 %. Highest ultimate tensile strength is achieved for Condition #9, while Conditions #6 and #8 are within 5% drop-off. Those results can be explained, on one hand as, Conditions #6 and #9 corresponded to full heating of the heatbed. On the other hand, Condition #8 also corresponds to the highest printhead temperature and the drop-off in UTS from 100 % to 50 % heatbed strategy is limited. Similarly, the conditions with 50 % heatbed strategy exhibit a limited drop-off in UTS compared

Table 5 Cost parameters held constant throughout the experiment. *Note : prices were converted into Euros according to the exchange rate on March 9 2022.*

Category	Parameters	Value	Source
Material	Base material part cost	52.78 EUR/500g	Supplier
Electricity	Base electricity cost	0.32 EUR/kWhr	Mean from public data [44]
Consumables	Printhead cost	227.49 EUR	Supplier
	Expected lifetime of printhead	1 year	Estimation from experience
	Heatbed cost	109.19 EUR	Supplier
	Expected lifetime of heatbed	1 year	Estimation from experience

**Fig. 3** The estimated manufacturing cost and cost distribution for each condition. *Note : Condition #1 is not represented.*

to their counterpart with 100 %. A lower ultimate tensile strength for other conditions (#2, #3, #4, #5 and #7) indicate that both printing parameters need to be optimized in order to achieved the highest resistance.

6 Discussion

The printhead temperature and the heatbed strategy were compared in three cost categories: materials, electricity, and consumables. The materials cost is the main source of cost and remained constant. Nonetheless, electricity cost is significant and was the most fluctuating of all three categories, ranging from 5 to 20% of the total cost. Moreover, electricity cost would increase for a longer duration of printing.

The change in total consumption according to the different parameters was as expected reflecting a total energy that was more than four times

higher when the heatbed was heated, increasing linearly across half and total heating. SEC and SPE underwent similar changes, as the temperature of the printhead and the heating strategy of the heatbed influenced both preparation power and fabrication power. Between the two parameters, the heatbed has the greater impact on energy consumption. Additionally, the unsuccessful printing in Condition #1 indicated a trade-off value or combination of the two parameters, determining the printability or otherwise of a part.

The results of tensile tests on the printed specimens also changed as expected: heating positively increased ultimate tensile strength. However, the change in strength between the different heating strategies was not linear. On one side a printing strategy of 0% for the heatbed considerably reduced tensile strength, 68% and 55% reduction compare to full heatbed strategy for printhead temperatures of 250 °C and 260 °C, respectively.

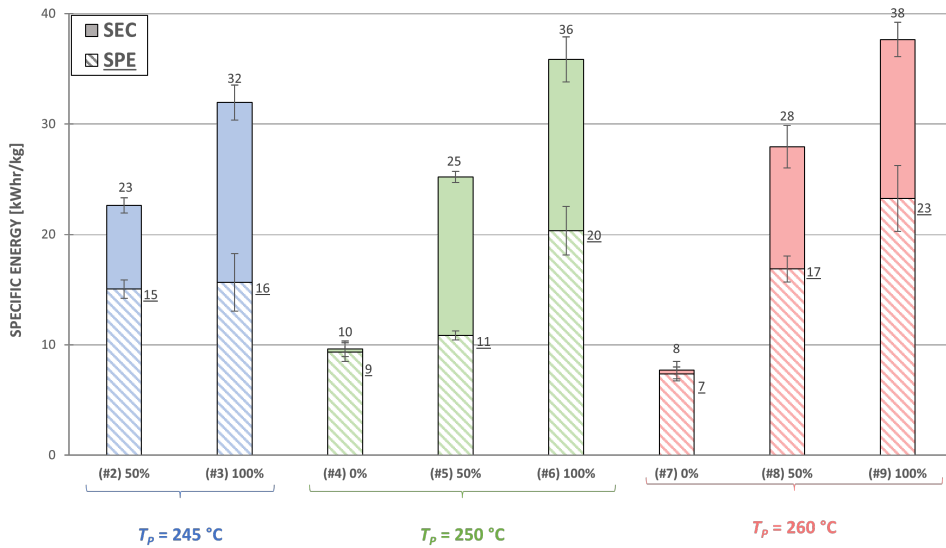


Fig. 4 Mean data for SEC and SPE for each experiment. Error bars correspond to 95% confidence interval. *Note : Condition #1 is not represented.*

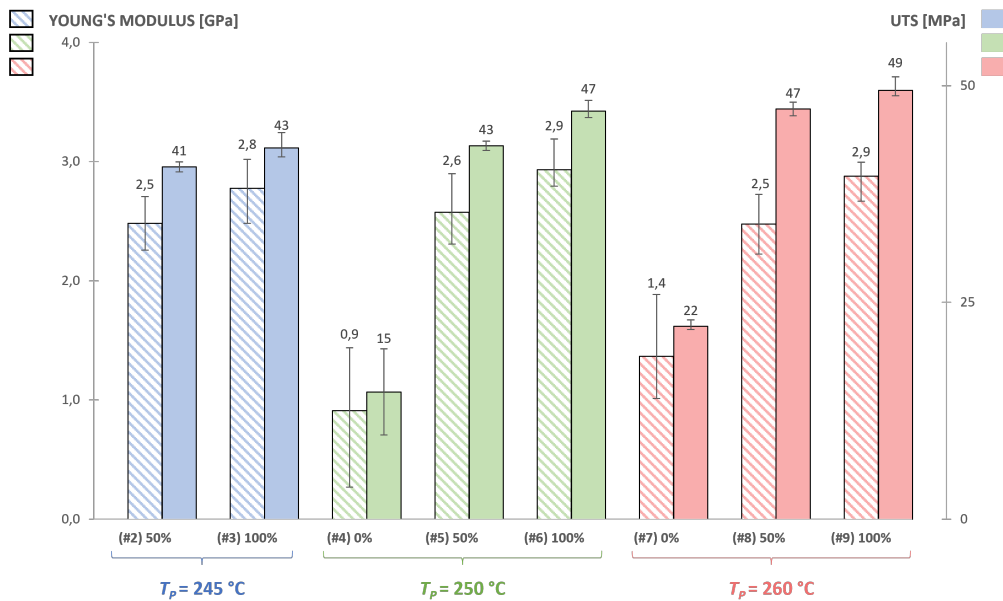


Fig. 5 Comparison of tensile modulus and UTS for each conditions. Error bars correspond to 95% confidence interval. *Note : Condition #1 is not represented.*

On the other side, the difference between a 50% strategy and full heating was relatively small, with 5% for 245 °C, 9% for 250 °C and 4% for 260 °C. Similarly for Young modulus, there are a 69% and 52% decreases between full and no heatbed heating for $T_p = 250$ °C and $T_p = 260$ °C. Between full and half heating, the drop-off are 11%, 10% and

14%, respectively. Additionally, conditions with same heatbed strategy (#4 and #7; #2, #5 and #8; #3, #6 and #9) present values of Young modulus within 0.1 GPa differences.

Figure 6 present each conditions regarding three main indicators : manufacturing cost, SPE and ultimate tensile strength. Such radar charts

ease comparison between different conditions. Condition #9 is the appropriate solution for a case where the highest mechanical performance is searched, as it exhibits the maximum UTS and Young's modulus. In the opposite case, conditions #4 and #7 are the cheapest and less energy consuming and are thus appropriate for cheap and energy scenario. Interestingly, the combination of 260 °C and half heating of the heatbed (condition #8) present a trade-off, being 4% less efficient on tensile resistance but offering a reduction of 28% in energy consumption and 3% in manufacturing cost. Depending on the targeted application, Condition #8 can thus be an appropriate compromise.

7 Conclusion

This work integrated emerging specific printing energy indicator to traditional cost and mechanical indicators in order to support decision-making in favor of more sustainable additive manufacturing. The aim of the present study was to develop an experimental method for gauging the impact of FFF printing parameters on three key indicators: manufacturing cost, specific printing energy, and ultimate tensile strength. Analysis of the flows involved in the process highlighted several economic variables as potential mean for optimization. To optimize the process in terms of cost and energy, both duration and power demand were identified as important variables. As duration is dependent on part design and desired mechanical strength, an optimization study would involve assessing both printing parameters and redesign. However, in the case of redesign the study would be case dependent thus harder to generalize.

By contrast, power demand is directly linked to printing parameters, making it much simpler to adjust for the operator. The present study therefore focused on a quick impact analysis of two parameters that influence the power demand for both the preparation phase and the printing phase: printhead temperature and heatbed heating strategy. With a relatively small design of experiments, an overview of all cost, energy and mechanical impacts can be estimated. Hence, the proposed methodology can be used to present solutions and strategies for optimizing the process, depending on the operator's requirements.

Future work would require to also investigate the duration variable, by evaluating parameters

such as deposition speed and layer thickness. Moreover measuring the interactions between all the parameters could also give a more precise idea of the ideal combination of parameters, depending on the situation. Regarding cost evaluation, taking full account of Eq. 1 with machine cost, especially in the case of production series would provide a more exhaustive view. Finally, the tensile strength and Young's modulus are not the only mechanical or technical indicators needed, as printing precision and surface roughness are key indicators in AM and need to be investigated further. Other mechanical tests, such as fatigue or flexural tests, could also be implemented and would be compatible with the proposed methodology.

Statements and Declarations

- Funding : The authors gratefully acknowledge the financial support from the Natural Sciences and Engineering Research Council of Canada through Discovery Grants program – Individual (NSERC) (RGPIN-4566-2018 NSERC) and financial support provided by Brittany Regional Council for the mobility of the PhD student.
- Conflict of interest/Competing interests : The authors have no relevant financial or non-financial interests to disclose.
- Availability of data and materials : The public data used for "Base electricity cost" in Table 5, were derived from the following resources available in the public domain : <https://mern.gouv.qc.ca/energie/statistiques-energetiques/prix-electricite/> [44]. Any other data that support the findings of this study are available on request from the corresponding author.
- Code availability : Not applicable
- Ethics approval : Not applicable
- Consent to participate : Not applicable
- Consent for publication : Not applicable
- Authors' contributions : All authors contributed to the study conception and design. Material preparation, data collection and analysis were performed by Thibault Le Gentil, Daniel Therriault and Olivier Kerbrat. The first draft of the manuscript was written by Thibault Le Gentil and all authors commented on previous versions of the manuscript. All authors read and approved the final manuscript. The authors

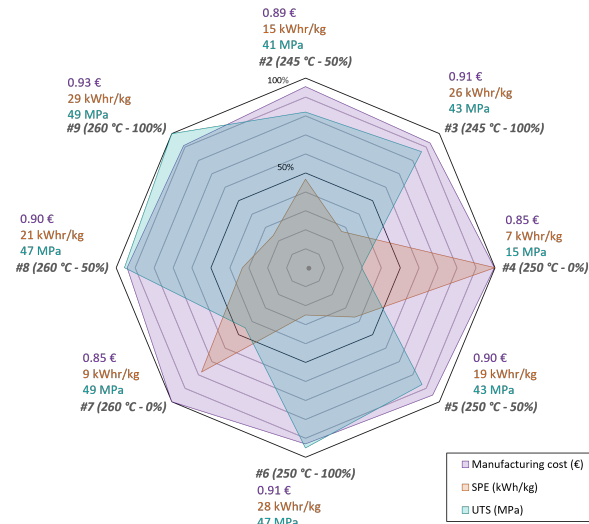


Fig. 6 Radar charts for Conditions 2-9. Values are normalized, 100% being the optimum value (maximum for ultimate tensile strength and minimum for total cost and SEC).

would also like to thank Sarah Benschir for her help on uncertainty quantification and tensile tests.

References

- [1] Wang X, Jiang M, Zhou Z, Gou J, Hui D. 3D printing of polymer matrix composites: A review and prospective. *Composites Part B: Engineering*. 2017;110:442–458. <https://doi.org/10.1016/j.compositesb.2016.11.034>.
- [2] Mabkhot MM, Ferreira P, Maffei A, Podrżaj P, Mądziel M, Antonelli D, et al. Mapping industry 4.0 enabling technologies into united nations sustainability development goals. *Sustainability (Switzerland)*. 2021;13(5):1–35. <https://doi.org/10.3390/su13052560>.
- [3] Ramalho A, Santos TG, Bevans B, Smoqi Z, Rao P, Oliveira JP. Effect of contaminations on the acoustic emissions during wire and arc additive manufacturing of 316L stainless steel. *Additive Manufacturing*. 2022;51(December 2021). <https://doi.org/10.1016/j.addma.2021.102585>.
- [4] Zuo X, Zhang W, Chen Y, Oliveira JP, Zeng Z, Li Y, et al. Wire-based directed energy deposition of NiTiTa shape memory alloys: Microstructure, phase transformation, electrochemistry, X-ray visibility and mechanical properties. *Additive Manufacturing*. 2022;59(PB):103115. <https://doi.org/10.1016/j.addma.2022.103115>.
- [5] Suárez L, Domínguez M. Sustainability and environmental impact of fused deposition modelling (FDM) technologies. *International Journal of Advanced Manufacturing Technology*. 2020;106(3-4):1267–1279. <https://doi.org/10.1007/s00170-019-04676-0>.
- [6] Paris H, Mokhtarian H, Coatanéa E, Museau M, Ituarte IF. Comparative environmental impacts of additive and subtractive manufacturing technologies. *CIRP Annals - Manufacturing Technology*. 2016;65(1):29–32. <https://doi.org/10.1016/j.cirp.2016.04.036>.
- [7] Tofail SAM, Koumoulos EP, Bandyopadhyay A, Bose S, Donoghue LO, Charitidis C. Additive manufacturing : scientific and technological challenges, market uptake and opportunities. *Materials Today*. 2018;21(1):22–37. <https://doi.org/10.1016/j.mattod.2017.07.001>.

- [8] van de Werken N, Tekinalp H, Khanbolouki P, Ozcan S, Williams A, Tehrani M. Additively manufactured carbon fiber-reinforced composites: State of the art and perspective. *Additive Manufacturing*. 2020;31(July 2019):100962. <https://doi.org/10.1016/j.addma.2019.100962>.
- [9] Herrmann C, Dewulf W, Hauschild M, Kaluza A, Kara S, Skerlos S. Life cycle engineering of lightweight structures. *CIRP Annals*. 2018;67(2):651–672. <https://doi.org/10.1016/j.cirp.2018.05.008>.
- [10] Rahim TNAT, Abdullah AM, Akil HM, Mohamad D, Rajion ZA. The improvement of mechanical and thermal properties of polyamide 12 3D printed parts by fused deposition modelling. *Express Polymer Letters*. 2017;11(12):963–982. <https://doi.org/10.3144/expresspolymlett.2017.92>.
- [11] Vidakis N, Petousis M, Kechagias JD. Parameter effects and process modelling of Polyamide 12 3D-printed parts strength and toughness. *Materials and Manufacturing Processes*. 2022;37(11):1358–1369. <https://doi.org/10.1080/10426914.2022.2030871>.
- [12] Griehl W, Ruestem D. Nylon-12-Preparation, Properties, and Applications. *Industrial & Engineering Chemistry*. 1970;62(3):16–22. <https://doi.org/10.1021/ie50723a005>.
- [13] Kausar A. Advances in Carbon Fiber Reinforced Polyamide-Based Composite Materials. *Advances in Materials Science*. 2019;19(4):67–82. <https://doi.org/10.2478/adms-2019-0023>.
- [14] Abderrafai Y, Hadi Mahdavi M, Sosa-Rey F, Hérard C, Otero Navas I, Piccirelli N, et al. Additive manufacturing of short carbon fiber-reinforced polyamide composites by fused filament fabrication: Formulation, manufacturing and characterization. *Materials and Design*. 2022;214:110358. <https://doi.org/10.1016/j.matdes.2021.110358>.
- [15] Ferreira I, Madureira R, Villa S, de Jesus A, Machado M, Alves JL. Machinability of PA12 and short fibre-reinforced PA12 materials produced by fused filament fabrication. *International Journal of Advanced Manufacturing Technology*. 2020;107(1-2):885–903. <https://doi.org/10.1007/s00170-019-04839-z>.
- [16] Ensinger Plastics.: TECAMID 12 natural Ensinger Plastics“. Available from: <https://www.ensingerplastics.com/en/shapes/products/pa12-tecamid-12-natural>.
- [17] Evonik.: Product Information VESTAMID® Care ML16. Available from: <https://www.plastics-database.com/material/pdf/VESTAMIDCareML16/VESTAMIDCareML16?sLg=en&rnd=1665067677760>.
- [18] Baba MN. Flatwise to Upright Build Orientations under Three-Point Bending Test of Nylon 12 (PA12) Additively Manufactured by SLS. *Polymers*. 2022;14(5). <https://doi.org/10.3390/polym14051026>.
- [19] Tomanik M, Zmudzińska M, Wojtków M. Mechanical and Structural Evaluation of the PA12 Desktop Selective Laser Sintering Printed Parts Regarding Printing Strategy. *3D Printing and Additive Manufacturing*. 2021;8(4):271–279. <https://doi.org/10.1089/3dp.2020.0111>.
- [20] Rahim TNAT, Abdullah AM, Md Akil H. Recent Developments in Fused Deposition Modeling-Based 3D Printing of Polymers and Their Composites. *Polymer Reviews*. 2019;59(4):589–624. <https://doi.org/10.1080/15583724.2019.1597883>.
- [21] Dickson AN, Barry JN, McDonnell KA, Dowling DP. Fabrication of continuous carbon, glass and Kevlar fibre reinforced polymer composites using additive manufacturing. *Additive Manufacturing*. 2017;16:146–152. <https://doi.org/10.1016/j.addma.2017.06.004>.
- [22] Chacón JM, Caminero MA, Núñez PJ, García-Plaza E, García-Moreno I, Reverte JM. Additive manufacturing of continuous fibre reinforced thermoplastic composites

- using fused deposition modelling: Effect of process parameters on mechanical properties. *Composites Science and Technology*. 2019;181(June):107688. <https://doi.org/10.1016/j.compscitech.2019.107688>.
- [23] Yan C, Hao L, Xu L, Shi Y. Preparation, characterisation and processing of carbon fibre/polyamide-12 composites for selective laser sintering. *Composites Science and Technology*. 2011;71(16):1834–1841. <https://doi.org/10.1016/j.compscitech.2011.08.013>.
- [24] Jansson A, Pejryd L. Characterisation of carbon fibre-reinforced polyamide manufactured by selective laser sintering. *Additive Manufacturing*. 2016;9:7–13. <https://doi.org/10.1016/j.addma.2015.12.003>.
- [25] Liao G, Li Z, Cheng Y, Xu D, Zhu D, Jiang S, et al. Properties of oriented carbon fiber/polyamide 12 composite parts fabricated by fused deposition modeling. *Materials and Design*. 2018;139:283–292. <https://doi.org/10.1016/j.matdes.2017.11.027>.
- [26] Blok LG, Longana ML, Yu H, Woods BKS. An investigation into 3D printing of fibre reinforced thermoplastic composites. *Additive Manufacturing*. 2018;22(March):176–186. <https://doi.org/10.1016/j.addma.2018.04.039>.
- [27] 3DXTech.: CarbonX™ Carbon Fiber Nylon 12 (PA12) 3D Filament. Available from: https://www.3dxtech.com/wp-content/uploads/2021/04/CF_PA12.v1.pdf.
- [28] Saade MRM, Yahia A, Amor B. How has LCA been applied to 3D printing? A systematic literature review and recommendations for future studies. *Journal of Cleaner Production*. 2020;244:118803. <https://doi.org/10.1016/j.jclepro.2019.118803>.
- [29] Lunetto V, Priarone PC, Galati M, Minetola P. On the correlation between process parameters and specific energy consumption in fused deposition modelling. *Journal of Manufacturing Processes*. 2020;56(June):1039–1049. <https://doi.org/10.1016/j.jmapro.2020.06.002>.
- [30] Elkaseer A, Schneider S, Scholz S. Experiment-Based Process Modeling and Optimization for High-Quality and Resource-Efficient FFF 3D Printing. *Applied Sciences*. 2020;.
- [31] Baumers M, Dufflou JR, Flanagan W, Gutowski TG, Kellens K, Lifset R. Charting the Environmental Dimensions of Additive Manufacturing and 3D Printing. *Journal of Industrial Ecology*. 2017;21:S9–S14. <https://doi.org/10.1111/jieec.12668>.
- [32] Kara S, Li W. Unit process energy consumption models for material removal processes. *CIRP Annals - Manufacturing Technology*. 2011;60(1):37–40. <https://doi.org/10.1016/j.cirp.2011.03.018>.
- [33] Liu Z, Jiang Q, Ning F, Kim H, Cong W, Xu C, et al. Investigation of energy requirements and environmental performance for additive manufacturing processes. *Sustainability (Switzerland)*. 2018;10(10). <https://doi.org/10.3390/su10103606>.
- [34] Dunaway D, Harstvedt JD, Ma J. A Preliminary Experimental Study of Additive Manufacturing Energy Consumption. *Proceedings of the ASME 2017 International Design Engineering Technical Conferences and Computers and Information in Engineering Conference*. 2017;p. 1–8.
- [35] Ma Z, Gao M, Wang Q, Wang N, Li L, Liu C, et al. Energy consumption distribution and optimization of additive manufacturing. *International Journal of Advanced Manufacturing Technology*. 2021;116(11-12):3377–3390. <https://doi.org/10.1007/s00170-021-07653-8>.
- [36] Ruckstuhl K, Costa Camoes Rabello R, Davenport S. Design and responsible research innovation in the additive manufacturing industry. *Design Studies*. 2020;71:100966. <https://doi.org/10.1016/j.destud.2020.100966>.
- [37] Freeman B, Coville D, Hicks D. Cost estimation of CNC vs composite reinforced FDM3D printing for low-volume production

of motorcycle components. *American Journal of Engineering, Science and Technology*. 2020;6:1–13.

- [38] Lunetto V, Priarone PC, Kara S, Settineri L. A comparative LCA method for environmentally friendly manufacturing: Additive manufacturing versus Machining case. *Procedia CIRP*. 2021;98:406–411. <https://doi.org/10.1016/j.procir.2021.01.125>.
- [39] Urbanic RJ, Saqib SM. A manufacturing cost analysis framework to evaluate machining and fused filament fabrication additive manufacturing approaches. *International Journal of Advanced Manufacturing Technology*. 2019;102(9-12):3091–3108. <https://doi.org/10.1007/s00170-019-03394-x>.
- [40] Ingarao G, Priarone PC. A comparative assessment of energy demand and life cycle costs for additive- and subtractive-based manufacturing approaches. *Journal of Manufacturing Processes*. 2020;56(June 2019):1219–1229. <https://doi.org/10.1016/j.jmapro.2020.06.009>.
- [41] Niaki MK, Torabi SA, Nonino F. Why manufacturers adopt additive manufacturing technologies: The role of sustainability. *Journal of Cleaner Production*. 2019;222:381–392. <https://doi.org/10.1016/j.jclepro.2019.03.019>.
- [42] Yosofi M, Kerbrat O, Mognol P. Additive manufacturing processes from an environmental point of view- a new methodology for combining technical, economic, and environmental predictive models. *The International Journal of Advanced Manufacturing Technology*. 2019;102(Section 2):4073–4085. <https://doi.org/10.1007/s00170-019-03446-2>.
- [43] Gutierrez-Osorio AH, Ruiz-Huerta L, Caballero-Ruiz A, Siller HR, Borja V. Energy consumption analysis for additive manufacturing processes. *International Journal of Advanced Manufacturing Technology*. 2019;105(1-4):1735–1743. <https://doi.org/10.1007/s00170-019-04409-3>.
- [44] Ministère de l'Énergie et des Ressources naturelles du Québec.: Prix de l'électricité. Available from: <https://mern.gouv.qc.ca/energie/statistiques-energetiques/prix-electricite/>.